



# Localized surface plasmon resonance (LSPR) biosensor based on thermally annealed silver nanostructures with on-chip blood-plasma separation for the detection of dengue non-structural protein NS1 antigen

Pearlson Prashanth Austin Suthanthiraraj, Ashis Kumar Sen\*

Department of Mechanical Engineering, Indian Institute of Technology Madras, Chennai 600036, India

## ARTICLE INFO

### Keywords:

Dengue  
NS1 antigen  
Localized surface plasmon resonance  
Silver nanostructures  
Plasma separation  
Polyethersulfone membrane

## ABSTRACT

Early diagnosis of dengue biomarkers by employing a technology that is less labor- and time-intensive and offers higher sensitivity and lower limits of detection would find great significance in the developing world. Here, we report the development of a biosensor that exploits the localized surface plasmon resonance (LSPR) effect of silver nanostructures, created via thermal annealing of thin metal film, to detect dengue NS1 antigen, which appears as early as the onset of infection. The biosensor integrates membrane-based blood-plasma separation to develop lab-on-chip device that facilitates rapid diagnosis (within 30 min) of dengue NS1 antigen from a small volume (10  $\mu\text{L}$ ) of whole blood. The refractive index (RI) sensitivity of the LSPR biosensor was verified by using aqueous glycerol (0–100 wt%) which showed that it is sufficiently sensitive to detect  $10^{-3}$  change in RI, which is comparable to that observed with protein-protein interaction. The RI sensitivity was utilized to demonstrate protein binding by using bovine serum albumin and detection of antibody-antigen immune reaction by binding human chorionic gonadotropin antigen to immunoglobulin antibody immobilized in our LSPR biosensor. Next, we demonstrated the detection of NS1 in plasma obtained via centrifugation and in plasma separated on-chip. From 10  $\mu\text{L}$  of whole blood spiked with NS1 antigen, our biosensor reliably detects 0.06  $\mu\text{g}/\text{mL}$  of NS1, which lies within the clinical limit observed during the first seven days of infection, with a sensitivity of 9 nm/ $(\mu\text{g}/\text{mL})$ . These results confirm that the proposed LSPR biosensor can potentially be used in point-of-care dengue diagnostics.

## 1. Introduction

Dengue is endemic and affects more than 100 million people annually. It is an infectious disease caused by four types of arboviruses, namely DENV-1, 2, 3 and 4, of the genus *Flavivirus*, and transmitted by adult female *Aedes aegypti* mosquito (Dengue, 2009). Currently, there is no targeted therapy for dengue, and patient treatment focuses on managing fluid losses by administering electrolytes. The common laboratory diagnosis methods for dengue include isolation of DENV in mosquito cell culture, inoculation of adult *Aedes aegypti* mosquito, detection of viral ribonucleic acid (vRNA) via polymerase chain reaction (PCR), detection of non-structural glycoprotein NS1 antigen secreted by viral plasmid or immunoglobulin antibodies IgG and IgM produced in response to dengue infection via enzyme linked immunosorbent assay (ELISA), or by a combination of these techniques (Pal et al., 2014; Peeling et al., 2010).

Although dengue biomarkers are abundant, the diagnostic

techniques utilized to identify these biomarkers suffer from certain limitations. For example, virus isolation is time-consuming (takes  $\sim 5$  days), less sensitive at low viral concentrations and prone to errors from virus-antibody complexes (Velez et al., 1984). While polymerase chain reaction (PCR) improves sensitivity via gene amplification, it requires sophisticated equipment and trained personnel for sample preparation and analysis (Lanciotti et al., 1992). In comparison, conventional ELISA is simple, and detects NS1 antigen and the immunoglobulin antibodies IgG and IgM. However, the assay is time-consuming (takes  $\sim 6$  h) and less sensitive for NS1 detection (Pal et al., 2014). To overcome these issues, alternate techniques were developed for dengue detection. By translating sandwich ELISA into disk format, the kinetics of antibody-analyte binding and sensitivity could be improved (Aeinehvand et al., 2015; Hosseini et al., 2015). However, binding was poor at large analyte concentrations, which limits its use for detecting mixed serotypes in endemic regions. Other approaches to improve sensitivity and specificity of conventional ELISA include embedding antibody-

\* Corresponding author.

E-mail address: [ashis@iitm.ac.in](mailto:ashis@iitm.ac.in) (A.K. Sen).

<https://doi.org/10.1016/j.bios.2019.02.036>

Received 29 November 2018; Received in revised form 5 February 2019; Accepted 15 February 2019

Available online 21 February 2019

0956-5663/ © 2019 Elsevier B.V. All rights reserved.

functionalized magnetic nanoparticles on a nitrocellulose strip (Ortega et al., 2017), conjugating affibodies screened against NS1 to gold nanoparticles (Bang et al., 2018), using microcolumns in a microfluidic chip (Weng et al., 2011), etc.

Furthermore, externally applied fields were also used to manipulate beads and virus for dengue immunoassays. To this end, magnetic nanoparticles were applied to virus separation and subsequent nucleic acid amplification (Patramool et al., 2013; Zaytseva et al., 2005). Using just 6  $\mu\text{L}$  of serum, magnetic nanoparticle clustering enabled detecting 25 ng/mL of NS1 in < 10 min (Antunes et al., 2015). Besides, dielectrophoresis of fluorescently-labelled, virus-conjugated silica beads was also employed to isolate and quantify dengue virus (Iswardy et al., 2017). Despite their utility, the use of magnetic nanoparticles and fluorescence probes increases the cost and annuls the potential benefits of these techniques.

Alternatively, rapid diagnostic tests (RDT's) utilizing immunochromatographic principles were developed (Blacksell, 2012). These devices consist of antibody-embedded nitrocellulose membrane. Generally, change in colour of the membrane upon sample flow confirms the presence of analyte. Although RDT's require low sample volumes and provide results in < 90 min, they are less sensitive than conventional ELISA.

To improve diagnostic accuracy, biosensors based on electrical (Fang et al., 2010; Hadis et al., 2017; Huang et al., 2013; Wasik et al., 2018), electrochemical (Avelino et al., 2014; Dias et al., 2013; Dutra et al., 2018; Navakul et al., 2017; Nguyen et al., 2012; Odeh et al., 2017; Oliveira et al., 2011; Ortega et al., 2018; Parkash et al., 2014; Silva et al., 2014, 2015; Souza et al., 2011) and optical (Darwish et al., 2018; Iswardy et al., 2017; Laguna et al., 2014; Mustapha Kamil et al., 2018a, 2018b; Sánchez-Purrà et al., 2017) sensing mechanisms were developed for dengue detection (Parkash and Shueb, 2015). The detection of analyte via electrical and electrochemical sensing mechanisms is characterized by change in current, potential difference, resistance, impedance and/or the voltage-current (V-I) characteristics of the antibody-immobilized electrode. Despite achieving limit of detection (LOD) in the clinical range, these techniques are too sensitive to pH of the buffer, limiting reproducibility. Such limitations can be overcome by using optical techniques, where ligand-receptor binding is characterized solely by change in the intensity of reflected, scattered and transmitted signal from optically active surfaces, nanoparticles, nanostructures, or fluorescence from microbeads. In recent years, optical detection techniques exploiting light-matter interactions such as surface plasmon resonance (SPR) (de Oliveira et al., 2017; Hu et al., 2013; Jahanshahi et al., 2015; Kumbhat et al., 2010; Omar et al., 2018), long range surface plasmon polariton (LRSP) (Wong et al., 2016, 2014), surface-enhanced Raman scattering (SERS) (Sánchez-Purrà et al., 2017) and localized surface plasmon resonance (LSPR) (Adegoke and Park, 2017; Camara et al., 2013) were developed for dengue detection. SPR permits real-time and label-free detection. However, it requires expensive equipment, which limits its use in resource-poor settings. A functionally similar but relatively less-complicated and inexpensive alternative is LRSP. LRSP's have longer sensing region than SPR. However, the fabrication of LRSP sensors is complex, limiting reproducibility. SERS and LSPR are characterized by enhanced electromagnetic field at the surface of metal nano-architectures, due to frequency-matched collective oscillation of electrons in the conduction band of the metal, upon incidence of light. While SERS requires conjugating reporter molecules to improve sensitivity, LSPR is truly label-free. Interestingly, LSPR of annealed gold nanoparticles was previously demonstrated to be sufficiently sensitive to detect 0.074  $\mu\text{g}/\text{mL}$  dengue NS1 antigen (Camara et al., 2013).

Among dengue biomarkers, only the viral RNA and NS1 antigen appear as early as the onset of infection. While viral RNA can be detected only via time-intensive cell culture or relatively expensive nucleic acid amplification techniques, the detection of NS1 is simple and is achieved by monitoring NS1 binding to its complementary antibody.

Furthermore, NS1 antigen can be used to detect all four dengue serotypes. Therefore, a highly sensitive mechanism capable of detecting minute amounts of NS1 will aid early diagnosis. Among the detection mechanisms previously tested for dengue, LSPR is a promising alternative to conventional dengue detection because it enables label-free detection, requires relatively less expensive optical components and low volume of reagents, and provides quantitative information about the analyte, thereby helping in identifying the stage of infection.

In this paper, we report a localized surface plasmon resonance (LSPR)-based biosensor for detecting NS1 antigen in whole blood. The biosensor developed herein was fabricated by thermally annealing thin silver film deposited onto silicon substrate. By using glycerol solutions of 0–100% weight concentration, we first determined the refractive index sensitivity of our biosensor to be  $10^{-3}$ . Next, after confirming the ability of our biosensor to detect the adsorption of bovine serum albumin (BSA) and binding of human chorionic gonadotropin antigen to immobilized immunoglobulin (IgG) antibody, we studied the detection of NS1 antigen spiked into plasma, varying in concentration by two orders of magnitude. Finally, we integrated a polyethersulfone membrane filter at the inlet of the biosensor, and successfully demonstrated on-chip separation of blood cells from plasma, and subsequent detection of NS1 antigen in the filtered plasma, by using just 10  $\mu\text{L}$  of NS1 spiked-whole blood. Our LSPR biosensor yields a sensitivity of  $\sim 9 \text{ nm}/(\mu\text{g}/\text{mL})$  and limit of detection (LOD)  $\sim 0.06 \mu\text{g}/\text{mL}$ , which lies within the clinical levels of NS1 observed during the first few days of dengue infection.

## 2. Material and methods

### 2.1. Materials

Silicon wafer was purchased from Semiconductor Technology and Applications, USA. Trichloroethylene, nitric acid, hydrofluoric acid (HF), 3-aminopropyltriethoxysilane (APTES), 11-mercapto undecanoic acid (MUA), 3-mercapto propionic acid (MPA), N-(3-dimethylamino-propyl)-N'-ethyl carbodiimide hydrochloride (EDC) and N-hydroxy succinimide (NHS) were purchased from Sigma Aldrich, USA. Acetone and isopropyl alcohol were purchased from Fisher Scientific, USA. Methanol was purchased from Finar, India. The elastomer Sylgard 184 and curing agent were purchased from Dow Corning, USA. Glycerol was purchased from Fisher Scientific, USA. Goat anti-mouse immunoglobulin (IgG) antibody and colloidal gold human chorionic gonadotropin (AuHCG) antigen were purchased from Advanced Microdevices, India. Bovine serum albumin (BSA packed with ab207002), anti-dengue virus NS1 glycoprotein antibody [DN3] (ab41616), recombinant dengue virus 2 NS1 glycoprotein antigen (ab64456) and 10 kDa spin column (ab93349) were purchased from Abcam, USA. The plasma separation membrane (PSM0180-A) was supplied by Cobetter Filtration, China.

### 2.2. Substrate metallization and thermal annealing

One-half of a 100 mm, P-type silicon substrate was used for metallization. First, the substrate was immersed sequentially in trichloroethylene, acetone and nitric acid, boiling at 180 °C for 4 min. Then, the substrate was immersed in hydrofluoric acid (HF) for 30 s, diluted 1:10 with deionized (DI) water. Next, 5 nm thick silver film was deposited via electron beam evaporation (BOC Edwards Auto 306, UK) at  $10^{-6}$  Torr. Then, the metal film was annealed inside a furnace at 200 °C for 1 h. The thickness of the silver film, and the temperature and time of annealing were chosen based on prior observations (Sreenivasan et al., 2013). Finally, the substrate was cooled to room temperature, and diced manually into rectangular pieces of two different dimensions – 2 cm  $\times$  0.5 cm for studies with plasma and 3.5 cm  $\times$  1 cm for studies with whole blood.

### 2.3. Surface functionalization

To bind proteins and antibody for LSPR biosensing, we adapted the functionalization protocol followed previously with gold nanoparticle assembly on glass surface (Rajesh et al., 2012), discussed in detail in the [Supplementary information](#).

### 2.4. Device fabrication

Two different devices were fabricated, one each for the detection of NS1 antigen spiked into plasma and whole blood. The devices were designed using AutoCAD software (Autodesk, USA). The device used for protein binding and NS1 detection in plasma consists of a 3 mm diameter cylindrical chamber having 6 mm long channels (300  $\mu\text{m}$  wide, 500  $\mu\text{m}$  height) on either side, whereas the device used with NS1 detection in whole blood consists of a 3 cm long rectangular channel of width 1 mm and height 100  $\mu\text{m}$ , having a 4 mm diameter cylindrical inlet. A poly (methyl methacrylate) (PMMA) master mold created via micro-milling (Mini-Mill/GX, Minitech, USA) was used to create the chamber device, whereas a SU-8 master mold created via photolithography was used to create the microchannel for NS1 detection in whole blood. The G-code required for micro-milling was generated using Lazycam software (Newfangled Solutions, USA). The channels were fabricated of poly dimethyl methoxy silane (PDMS) via soft lithography from the master mold by following standard protocols (McDonald and Whitesides, 2002). Briefly, the elastomer and curing agent were mixed in the ratio of 10:1, de-aerated in the desiccator, and cured over a hot plate for 90 min at 70  $^{\circ}\text{C}$ . Next, the cured PDMS slab was treated in oxygen plasma (Harrick Plasma) maintained at 10 W for 2 min, together with the functionalized substrate. Finally, within a minute of plasma treatment, the cured PDMS slab was bonded to the substrate.

### 2.5. Experimental setup

The experimental setup comprises a deuterium-halogen light source (DH-2000-BAL, Ocean Optics, Germany), a reflection probe (QR-400-7-UV-VIS, Ocean Optics, Germany), a miniature spectrometer (Flame-T, Ocean Optics, Germany), and translation stages (Thor Labs, USA) (Fig. 1). The reflection probe consists of a fiber optic coupler, which permits transmitting light from the lamp to the substrate and the reflected light from the substrate to the spectrometer. Absorbance spectrum was acquired using OceanView software (Ocean Optics, Germany) installed in a Windows laptop. The integration time, number of scans and boxcar width were set to 15 ms, 25 and 50 respectively, and the spectra were corrected for nonlinearity errors. For spectral acquisition,

the separation between the reflection probe and the device was adjusted to be 3 mm by carefully adjusting the z-translation stage. Since the beam diameter equals half the separation distance, our system interrogates the LSPR substrate with a 1.5 mm circular beam.

### 2.6. Protocol for measurement of Refractive Index (RI) Sensitivity, Adsorption of Bovine Serum Albumin (BSA) and detection of antibody-antigen binding

The procedure adopted for determining refractive index sensitivity using glycerol solutions, adsorption of bovine serum albumin (BSA) and detection of antibody-antigen binding are described in detail in the [Supplementary information](#).

### 2.7. Protocol for detection of dengue NS1 antigen in plasma

The detection of dengue in plasma was demonstrated using the microchamber. The anti-NS1 antibody was diluted 1:10 in PBS. Dengue NS1 antigen of concentration ranging from 1 to 50  $\mu\text{g}/\text{mL}$  was prepared in plasma, acquired via centrifugation of healthy adult blood. The region of the chamber was selectively functionalized and incubated with anti-NS1 antibody for 3 h at 4  $^{\circ}\text{C}$ . After washing with PBS to remove unbound antibody, the substrate was incubated with 100  $\mu\text{g}/\text{mL}$  of BSA to prevent non-specific binding. Next, after removing unbound BSA by washing with excess PBS, the substrate was incubated with 30  $\mu\text{L}$  of plasma containing NS1 antigen for 3 h at 4  $^{\circ}\text{C}$ . Care was taken to minimize human exposure to NS1 antigen and the experimental area was disinfected periodically by using 10% sodium hypochlorite solution and 70% ethanol. A control experiment was conducted using plasma containing no spiked NS1 antigen. Absorbance spectrum was acquired thrice for each sample, the experiment was repeated at least thrice for each concentration of NS1 i.e. for each experiment, freshly prepared NS1 sample was pipetted into a newly fabricated microchamber device (immobilized with anti-NS1), and the mean and standard deviation of peak absorbance wavelength shift before and after NS1 incubation was computed.

### 2.8. Protocol for detection of dengue NS1 antigen in whole blood

The detection of NS1 antigen in plasma derived on-chip from whole blood was demonstrated in a rectangular PDMS channel having 4 mm diameter cylindrical inlet. For the separation of plasma from whole blood, a 5 mm  $\times$  5 mm polyethersulfone membrane, cut from an A4 size membrane pad, was used. The membrane is 340  $\mu\text{m}$  thick, and consists of asymmetrically-distributed 1.8  $\mu\text{m}$  pores, which is sufficient to retain red-, white blood cells and platelets, and permit high recovery

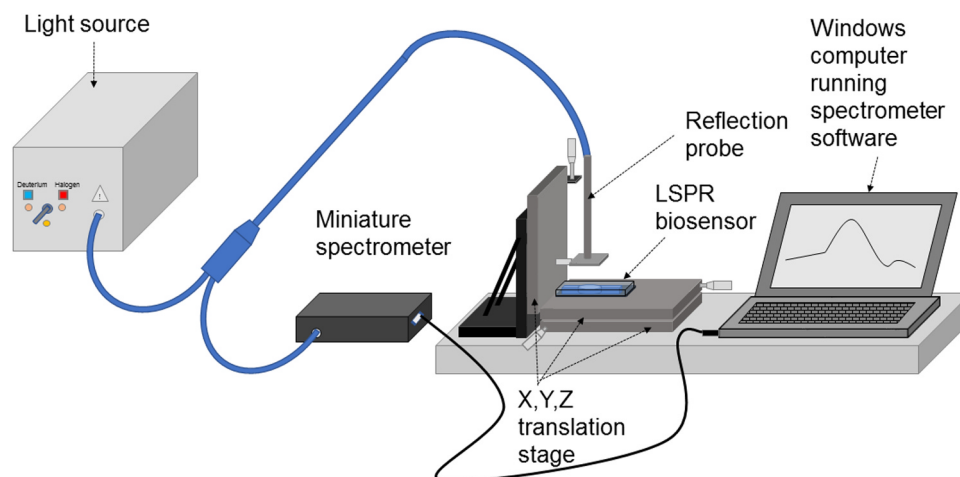


Fig. 1. Schematic of the experimental setup used for localized surface plasmon resonance (LSPR) sensing.

of plasma from at most  $35 \mu\text{L}/\text{cm}^2$  of whole blood. The anti-NS1 antibody was diluted 1:10 in PBS, and dengue NS1 antigen was diluted in whole blood, acquired from healthy adult, to the desired concentration ranging from 0.25 to  $2 \mu\text{g}/\text{mL}$ . A  $0.75 \text{ cm} \times 1 \text{ cm}$  region at one end of the diced substrate was selectively functionalized to bind anti-NS1 antibody and was used as the sensing region. For NS1 detection, the sensing region was first incubated with  $50 \mu\text{L}$  of anti-NS1 antibody (Abcam, USA). After PBS wash to remove unbound antibody, the free/unbound sites were blocked by incubation with  $50 \mu\text{L}$  of BSA overnight at  $4^\circ\text{C}$ . Unbound BSA was removed the following day in another PBS wash step. Next, the PDMS slab containing the rectangular channel and its shallow inlet was bonded to the substrate only after antibody incubation and BSA blocking steps. Just prior to whole blood sample injection, the plasma separation membrane was quickly treated with  $35 \mu\text{L}$  of heparin for  $\sim 15 \text{ s}$  and bonded to the channel inlet. Next,  $10 \mu\text{L}$  of whole blood spiked with dengue NS1 antigen was pipetted onto the membrane, such that plasma separates and flows through the channel into the sensing region via capillary force. The device was then allowed to incubate with the separated plasma containing dengue NS1 antigen for 30 min at  $4^\circ\text{C}$ . After antigen incubation, the PDMS cover was peeled carefully and the substrate was washed repeatedly with excess PBS to remove traces of plasma and unbound antigen from the sensing region and the channel. A control experiment was conducted using healthy whole blood, i.e. without spiked NS1 antigen. For each device, absorbance spectrum was acquired from the sensing region after incubation with anti-NS1 antibody, after BSA blocking and after incubation with dengue NS1 antigen. Three spectral measurements were acquired for each sample, the experiment was repeated thrice for each concentration of NS1, and the mean and standard deviation were computed.

### 3. Results and discussion

#### 3.1. Creation of metal nanostructures

The creation of silver nanostructures via thermal annealing of thin silver film occurs due to thermodynamic instability of such films deposited under vacuum. The nanostructures are formed due to repeated recrystallization that occurs by virtue of low surface energy of the thin silver film. In this work, 5 nm silver film was deposited via E-beam evaporation, and silver nanostructures were generated after thermally annealing the film at  $200^\circ\text{C}$  for 1 h inside a furnace. Fig. 2 shows high resolution scanning electron microscopy (HRSEM) images of these silver nanostructures. As observed clearly in Fig. 2c, the silver nanostructures are almost spheroidal in shape, vary in dimension from  $\sim 20$  to 80 nm, and have inter-structural spacing ranging from few tens to about a hundred nanometres. These structures exhibited peak absorbance at  $\sim 430 \text{ nm}$ , which conform to that of silver nanospheres of similar diameter (Tani, 2015).

In comparison to the prior approach (Camara et al., 2013), our biosensor presents certain advantages. First, silver inherently produces

large wavelength shifts than gold by virtue of (a) low electromagnetic damping losses due to low value of the imaginary part of the dielectric constant of silver, and (b) large variation of the real part of the dielectric constant in the visible region of the electromagnetic spectrum (Mayer and Hafner, 2011). Second, using silicon substrate as the base material allows fabricating single-use biosensors on a large scale, and also to retrieve the biosensor by suitable chemical treatment.

#### 3.2. Measurement of Refractive Index (RI) Sensitivity, Adsorption of Bovine Serum Albumin (BSA) and detection of antibody-antigen binding

The results for the Refractive Index Sensing using Glycerol Solutions, Adsorption of Bovine Serum Albumin (BSA) and Detection of antibody-antigen binding are presented and discussed in the [Supplementary information](#).

#### 3.3. Detection of dengue NS1 antigen in plasma

The dengue NS1 antigen appears as early as the zeroth day of infection and is therefore an effective biomarker for early diagnosis and subsequent treatment. Usually, the concentration of NS1 antigen in human blood varies from  $0.04$  to  $2 \mu\text{g}/\text{mL}$  up to 7 days of infection, and could be as high as  $50 \mu\text{g}/\text{mL}$  in certain cases (Alcon et al., 2002). Measurement of refractive index (RI) of three (3) independent samples of plasma containing  $100 \mu\text{g}/\text{mL}$  anti-NS1 with 0.5, 1 and  $2 \mu\text{g}/\text{mL}$  NS1 respectively, using a hand-held refractometer, showed RI values ranging from 1.348 to 1.350. This corresponds to  $\sim 10^{-3}$  variation in RI, which is sufficient to produce discrete wavelength shifts when analyzed via our biosensor. To demonstrate the ability of our biosensor to detect clinical levels of NS1 antigen, we diluted NS1 in plasma with concentration ranging from 0.5 to  $50 \mu\text{g}/\text{mL}$  and captured it over anti-NS1 antibody immobilized to silver nanostructures. Fig. 3 shows the absorbance spectra acquired after anti-NS1 immobilization and after NS1 capture for 0.5, 5 and  $50 \mu\text{g}/\text{mL}$  of NS1. While an increase in absorbance was observed at all concentrations confirming antigen binding, the trend in the peak wavelength shift was different. For the highest concentration, i.e.  $50 \mu\text{g}/\text{mL}$ , a large (108 nm) red-shift was observed, whereas for the lowest concentration of  $0.5 \mu\text{g}/\text{mL}$  NS1, a relatively moderate (6 nm) blue-shift was observed. Furthermore, even for  $2 \mu\text{g}/\text{mL}$ , which is the upper limit of NS1 in the early stage of infection, a blue-shift in the peak wavelength was observed relative to that after anti-NS1 immobilization. Regression analysis on fitting a linear line to the observed trend of wavelength shift with variation of dengue NS1 concentration provided an  $R^2 = 0.87$ . For the data in Fig. 3b, the wavelength shift up to  $2 \mu\text{g}/\text{mL}$  NS1 represents the average of five (5) discrete measurements from five (5) different microchamber devices, whereas for  $5 \mu\text{g}/\text{mL}$  and above, the data are from three (3) discrete measurements acquired similarly. The large error bars observed in Fig. 3b may be attributed to potential variation in fabrication conditions, which give rise to varying nanoparticle dimensions, spacing etc.

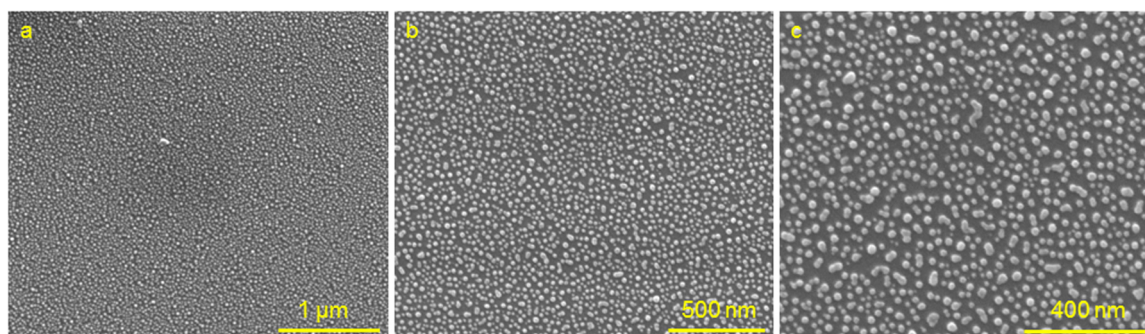
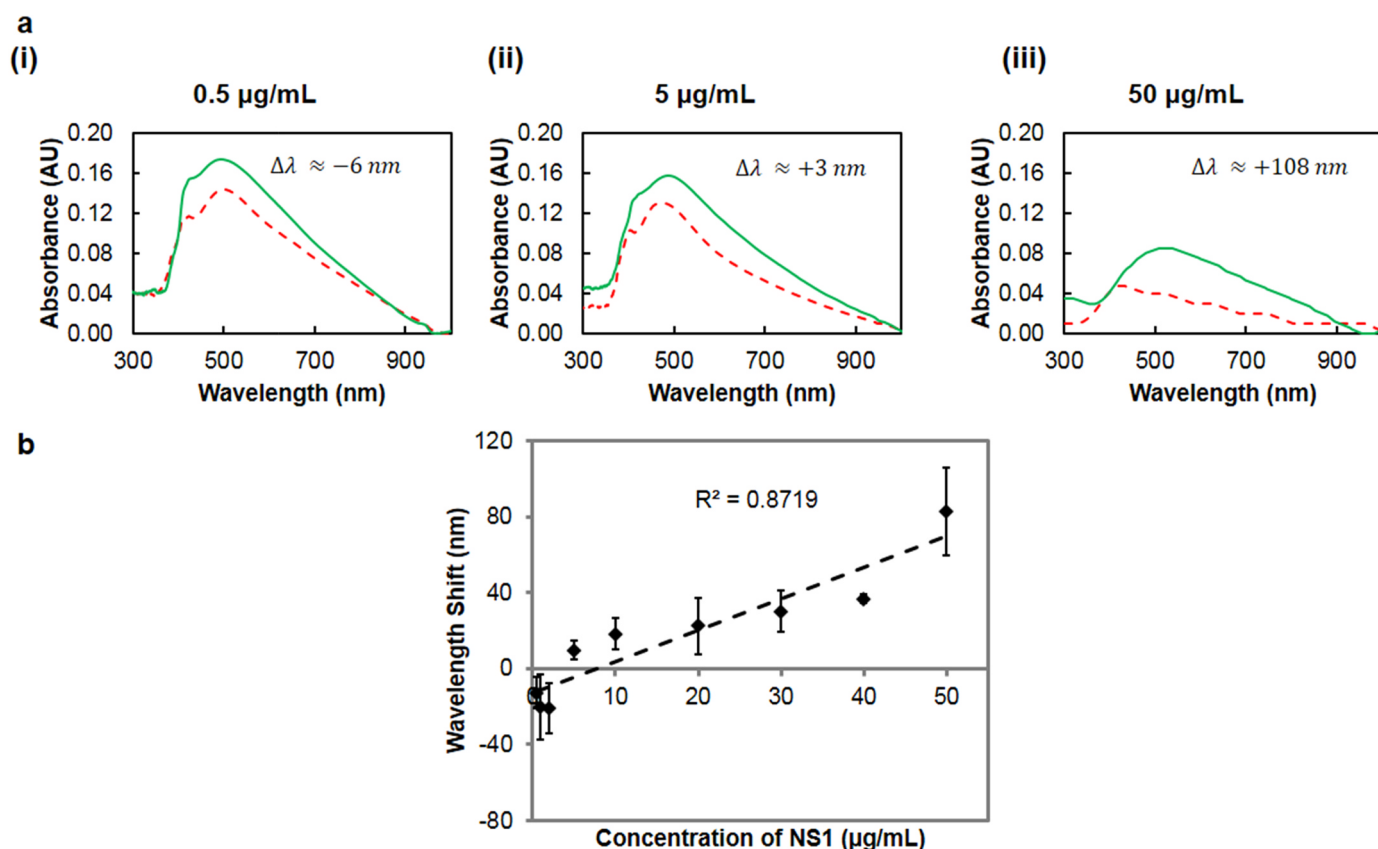


Fig. 2. High resolution scanning electron microscopy (HRSEM) images of silver nanostructures created via thermal annealing at (a)  $80,000 \times$ , (b)  $150,000 \times$  and (c)  $250,000 \times$ .



**Fig. 3.** Detection of dengue NS1 antigen in plasma (a) Absorbance spectra showing wavelength shift of absorbance maximum after incubation of silver nanostructures conjugated with anti-NS1 antibody (red dashed line) in the chamber device with (i) 0.5, (ii) 5 and (iii) 50 µg/mL of NS1 antigen (green solid line) (b) Plot of variation of wavelength shift of absorbance maximum with NS1 antigen concentration showing linearity with an  $R^2$  value of 0.87. (For interpretation of the references to color in this figure legend, the reader is referred to the web version of this article).

The relatively poor linearity observed herein is possibly due to the wide range of NS1 concentrations being investigated in our study, unlike most prior studies that were limited to 2 µg/mL at most (Bang et al., 2018; Camara et al., 2013; Dutra et al., 2018; Parkash et al., 2014). In comparison, for the control experiment conducted without suspending NS1 in plasma, we observed a mean shift of  $-8.37 \pm 2.22 \text{ nm}$ , accompanied by a small increase (0.003 AU) in absorbance (Fig. S7). Such significant shift in the absence of NS1 antigen can possibly be attributed to the interaction of serum albumin in plasma with unbound sites on silver nanostructures. The limit of detection (LOD) was determined as (Dutra et al., 2018)

$$\text{LOD} = \frac{3 \times \text{Standard deviation of control w/o antigen}}{\text{Slope of the linear fit for wavelength shift vs. NS1 concentration plot}} \quad (1)$$

The slope of the linear fit in Fig. 3b, which is  $\sim 1.87 \text{ nm}/(\mu\text{g/mL})$ , provides the sensitivity of NS1 detection in plasma obtained via centrifugation. By substituting the value of standard deviation of wavelength shift for the control experiment (i.e. 2.22 nm) into Eq. (1), we determined the LOD for NS1 in plasma to be  $\sim 4 \mu\text{g/mL}$ . However, if we limit our analysis to NS1 concentrations up to 5 µg/mL, the sensitivity increases to  $\sim 6 \text{ nm}/(\mu\text{g/mL})$ , and LOD to 1.1 µg/mL. Such improvement in sensitivity and LOD upon reduction of concentration range suggests potential interaction of plasma proteins with NS1. In our study, we observed blue shifts at low antigen concentrations (up to 2 µg/mL), similar to prior work on NS1 detection via LSPR (Camara et al., 2013). However, above 5 µg/mL NS1, the peak absorbance shifted increasingly towards red. Such concentration-dependent shifts may be attributed to several reasons, which include (i) randomly distributed nanostructures which gives rise to broad absorption spectrum having reduced intensity due to minimized constructive interference of scattered radiation

between nanostructures (Jenkins et al., 2014), (ii) low effective refractive index ( $n_{\text{eff}}$ ) due to sensing in air, which has low value of refractive index (1.003) in comparison to liquid media (1.33 or higher) used in most prior studies (Jenkins et al., 2014; Wang and Pan, 2008), (iii) strong adsorption of excess sulphur atoms in thiol groups of 11-MUA and 3-MPA to silver nanostructures, resulting in increased electromagnetic coupling (Henglein and Meisel, 1998), and (iv) variation in charge carrier accumulation within the semiconductor (i.e., silicon used as substrate for our LSPR biosensor) depending upon bound NS1 concentration, i.e. lower the NS1 concentration, the greater is the charge carrier accumulation giving rise to increased blue-shifts and vice versa (Fauchaux et al., 2014).

#### 3.4. On-chip blood-plasma separation and detection of dengue NS1 antigen in the separated plasma

Most existing dengue diagnostic techniques require processing infected blood samples manually to separate serum containing NS1 antigen via centrifugation (Parkash and Shueb, 2015). Despite its ubiquity, centrifugation is prone to red blood cell (RBC) lysis, which could interfere with signal sensitivity in medical diagnostics. Besides, centrifugation could deplete NS1 in blood, i.e. NS1 could be separated out into the cell fraction, resulting in false negative results (Cadamuro et al., 2018). Also, diagnostic devices that are capable of processing blood sample on-chip and yielding information regarding the possibility and stage of infection enable point-of-care applications. Toward this aim, we have demonstrated on-chip separation of plasma from whole blood and subsequent detection of NS1 antigen in the separated plasma by using polyethersulfone membrane, that permits plasma separation via gravity filtration, at the channel inlet. The membrane consists of

asymmetrically placed pores of size 1.8  $\mu\text{m}$ , which is sufficient to retain the blood cells. Previously polyethersulfone (or polysulfone) membrane was shown to minimize RBC lysis and retain 95% virus spiked into whole blood for downstream analysis (Liu et al., 2013). For these reasons, we used the polysulfone membrane-based blood-plasma separator with our LSPR biosensor for the detection of NS1 antigen spiked into whole blood. After repeated testing using membranes cut manually into different sizes and using different sample volumes, we found that 5 mm  $\times$  5 mm membrane dimension and 10  $\mu\text{L}$  whole blood are ideal for separating plasma in our biosensor. Furthermore, channel hydrophilicity played an important role in plasma separation, and subsequently, the capillary flow of separated plasma through the channel. For successful blood-plasma separation, the waiting time between oxygen plasma treatment and PDMS channel bonding was found to be critical. After prolonged waiting times ( $> 15$  min), plasma was found to be retained at the channel inlet and its capillary flow through the channel was impeded due to change in channel hydrophilicity (Fig. S9). For this reason, the PDMS slab was bonded to the annealed silver substrate just prior to NS1 antigen detection step, which was conducted within 3 min of bonding.

To demonstrate the separation of plasma from whole blood using the membrane, we bonded the PDMS channel to a glass slide and acquired images of the flow of extracted plasma using an inverted microscope. Fig. 4a and 4b show the schematic of the biosensor and the separation of plasma from infected whole blood using the polyethersulfone membrane. Just prior to separation, the membrane was treated quickly with heparin to minimize coagulation of blood cells on the filter and its influence on plasma yield. Fig. 4c clearly shows the advancement of plasma meniscus through the channel after separation. Using 5 mm  $\times$  5 mm membrane dimension and 10  $\mu\text{L}$  whole blood, the separated plasma was able to fill the channel including the sensing region within 30 s. From the analysis of gray scale intensity images acquired with and without plasma in Fig. S10, it is evident that the plasma separated using polyethersulfone membrane has higher purity than that separated via centrifugation.

Based on our observation of poor linearity at high NS1 concentrations, we limited the concentration range for analysis using our membrane-integrated biosensor to 0.25–2  $\mu\text{g}/\text{mL}$ . Fig. 4d shows the absorbance spectra for 0.25 and 2  $\mu\text{g}/\text{mL}$  of NS1 spiked into undiluted whole blood. In general, the shift in peak absorption wavelength was found to increase proportionally with NS1 concentration. However, such trend was not observed for absorbance values, just as in NS1 detection in plasma. While a red-shift of 5 nm was observed upon binding of 0.25  $\mu\text{g}/\text{mL}$  NS1, a shift of 28 nm was observed with 2  $\mu\text{g}/\text{mL}$  NS1. For the control experiment using NS1-free whole blood, we observed wavelength shift of  $2.98 \pm 0.17$  nm (Fig. S11). Upon regression analysis for the variation of peak absorbance wavelength shift with NS1 concentration, we observed a moderate linearity with  $R^2 = 0.84$  (Fig. 4e). The sensitivity and limit of detection (LOD) determined as above yielded values of 9.2 nm/( $\mu\text{g}/\text{mL}$ ) and 0.06  $\mu\text{g}/\text{mL}$  respectively. The sensitivity observed herein is comparable with that observed in prior study using NS1 antigen (Camara et al., 2013).

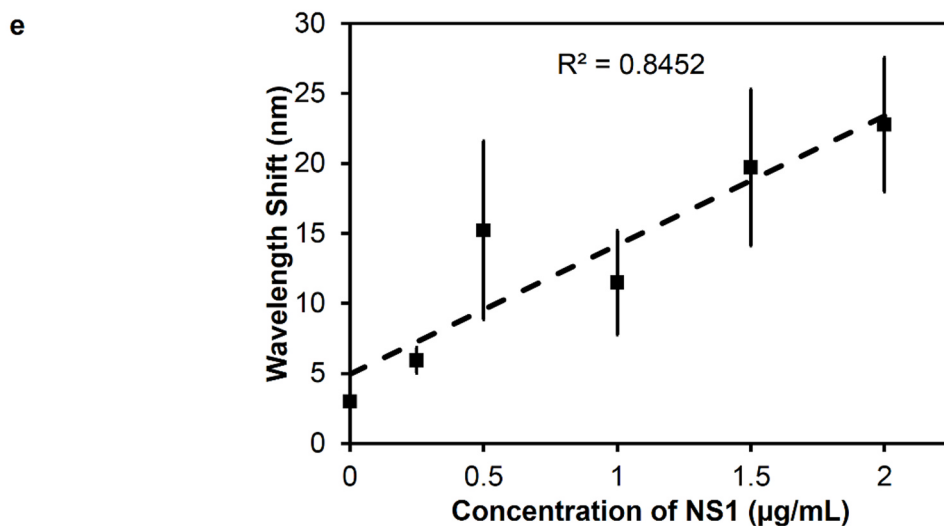
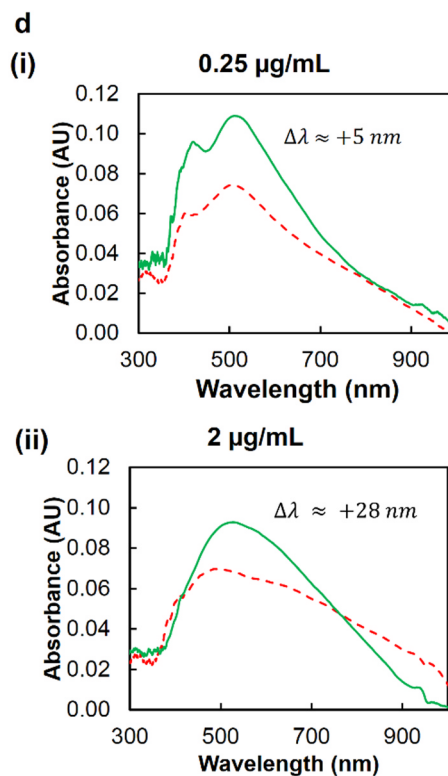
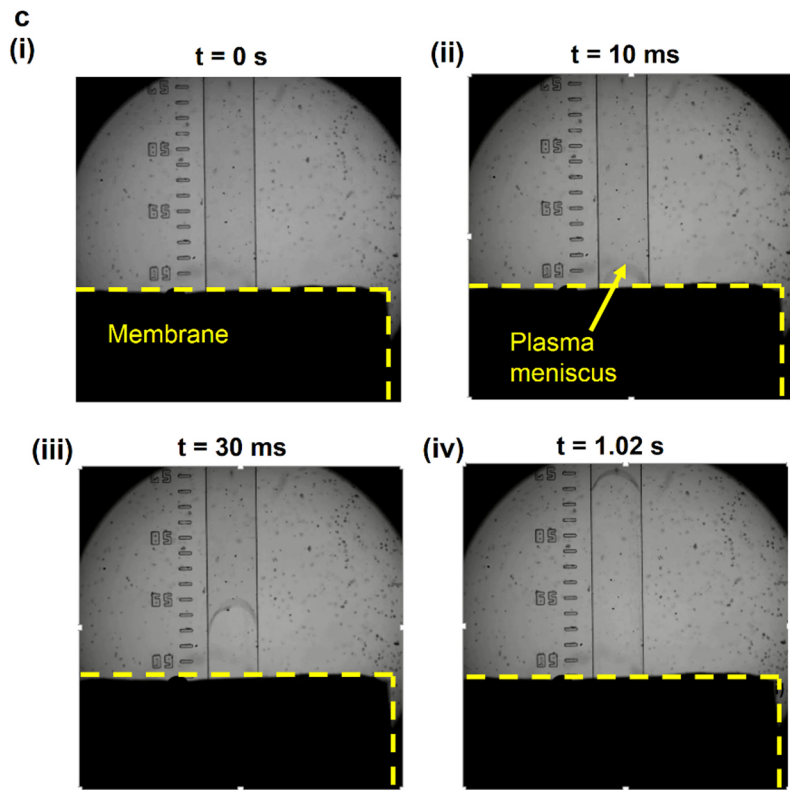
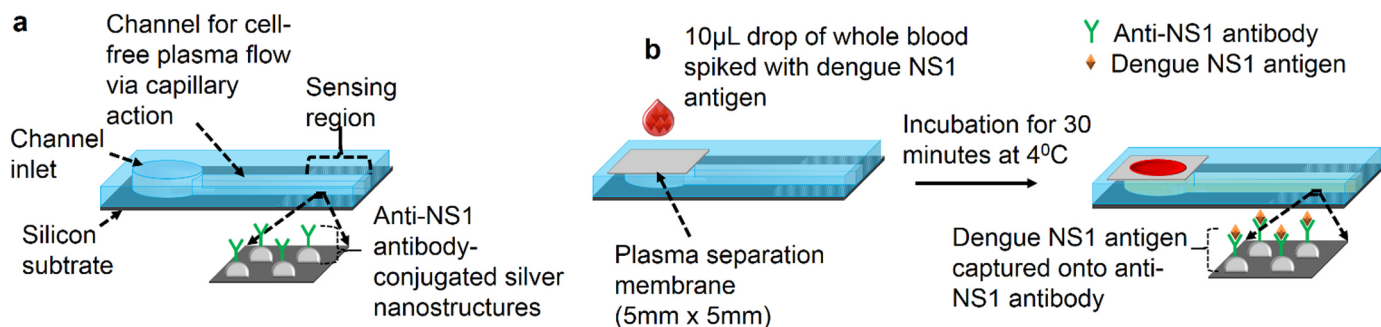
In comparison to Fig. 3b, Fig. 4e shows approximately 1-fold higher sensitivity. Such improved sensitivity may be attributed to the higher areal density of the bound NS1 antigen in the 1 mm  $\times$  0.75 cm sensing region of the rectangular channel, in comparison to the 3 mm microchamber, where NS1 will be sparsely distributed due to flow expansion inside the chamber. Furthermore, the smaller sensing region permits complete illumination of the sensing region due to similarity in dimensions of the beam spot and channel width, unlike the chamber where the chamber diameter is twice ( $2 \times$ ) the beam diameter. Also, in comparison to centrifugation, plasma obtained via filtration through the plasma separation membrane is anticipated to have higher purity, as the former is prone to contamination by platelets that interfere with NS1 binding. In the rectangular channel biosensor, platelets that measure 2–3  $\mu\text{m}$  in size will be retained within the 1.8  $\mu\text{m}$  pores of the

membrane. Besides improving sensitivity, the increased areal density of the bound NS1 antigen also contributes to the red-shift observed throughout in the 0–2  $\mu\text{g}/\text{mL}$  range of NS1, unlike the microchamber where blue-shift was observed for the same concentration range.

While one might anticipate that the broad absorbance peaks would reduce the resolution of wavelength shift due to variation in size of the nanostructures in a given sensor, we observed LOD that is comparable to a few prior studies (Antunes et al., 2015; Bang et al., 2018; Camara et al., 2013; Dutra et al., 2018; Odeh et al., 2017; Parkash et al., 2014; Sánchez-Purrà et al., 2017; Silva et al., 2015), and falls within the range (0.04–2  $\mu\text{g}/\text{mL}$ ) for early diagnosis. Although our data demonstrates low LOD for our LSPR biosensor, the linearity between wavelength shift and NS1 concentration is quite poor (i.e.  $R^2 < 0.9$ ). Since we acquired absorbance spectrum from a newly fabricated LSPR device for each measurement and for each NS1 concentration under investigation, such poor fit may be attributed to batch-to-batch variation in nanostructure size, spacing, areal density of immobilized anti-NS1 and bound NS1 antigen etc. Furthermore, it must be noted that none of the previous studies integrated sample preparation on chip, but instead used centrifuged plasma. The proposed device facilitates rapid diagnosis of dengue NS1 antigen within 30 min in contrast to 90 min required for the centrifuged plasma case. Moreover, while the volume of blood required for the study presented in Section 3.2 was 1 mL, only 10  $\mu\text{L}$  of blood was required in the present study. Therefore, the blood-plasma separation-integrated LSPR biosensor presented herein is an advancement in the field of dengue diagnostics with potential applications in point-of-care analysis.

#### 4. Conclusion

We have reported a biosensor that exploits the localized surface plasmon resonance (LSPR) effect of silver nanostructures, created via thermal annealing of thin metal film, to detect dengue NS1 antigen, which appears as early as the onset of infection. Our biosensor provides refractive index sensitivity of  $10^{-3}$ , and detects dengue NS1 antigen specifically over two-fold concentration range in plasma. By integrating the proposed biosensor with membrane-based blood-plasma separation, we have developed a lab-on-chip device that facilitates rapid diagnosis of NS1 (within 30 min) from just 10  $\mu\text{L}$  of whole blood. Besides reducing sample volume and assay time, our biosensor could potentially lower the assay cost also, as metal deposition and annealing are performed in bulk, and multiple biosensors can be fabricated from a single substrate. Furthermore, our biosensor reliably detects 0.06  $\mu\text{g}/\text{mL}$  of NS1, which lies within the clinical limit observed during the first seven days of infection, with a sensitivity of 9 nm/( $\mu\text{g}/\text{mL}$ ). However, the limit of detection above is based solely on calculations from wavelength shifts verified experimentally for NS1 concentrations  $> 0.25$   $\mu\text{g}/\text{mL}$ . The variation in size of the nanostructures gives rise to broad absorbance spectrum, which limits the resolution of wavelength shift that is critical to experimentally verifying low levels of NS1. Furthermore, the change in absorbance is small for NS1 concentration intervals in our study. For these reasons, our biosensor could only be used to qualitatively predict dengue infection (i.e., whether a person is infected or not) in its current form, but not to identify the stage of infection which is essential to initiate appropriate therapy. Nevertheless, our LSPR biosensor could be used as a rapid diagnostic test to diagnose dengue soon upon infection. Future work will focus on optimizing annealing parameters and utilizing substrates other than silicon to minimize charge carrier accumulation that could interfere with sensitivity. To improve resolution and to be able to experimentally verify the detection of NS1 antigen down to ng/mL concentration, we plan to generate more uniform metal nanostructures by using high annealing temperature and shorter annealing time. Upon optimization, we will validate our biosensor by testing dengue-infected patient samples.



(caption on next page)

**Fig. 4.** On-chip separation of blood cells from plasma and detection of NS1 antigen in the extracted plasma. (a) Schematic of the biosensor used with on-chip separation and detection of NS1 (b) Schematic showing the separation of blood cells from plasma using polyethersulfone membrane and the detection of dengue NS1 antigen in the extracted plasma (c) Time-sequence images acquired at (i)  $t = 0$  s, (ii)  $t = 10$  ms, (iii)  $t = 30$  ms and (iv)  $t = 1.02$  s showing the flow of extracted plasma as visualized by the capillary flow-based advancement of plasma meniscus through the rectangular channel after filtration of blood cells at the channel inlet. The yellow dotted lines indicate the boundary of the membrane attached on top of the inlet chamber. (d) Absorbance spectra acquired from the sensing region immobilized with anti-NS1 antibody (red dashed line) exhibiting wavelength shift of peak absorbance after incubation with plasma separated on-chip from whole blood samples containing (i) 0.25 and (ii) 2  $\mu\text{g}/\text{mL}$  of dengue NS1 antigen (green solid line). (e) Plot of variation of wavelength shift with concentration of NS1 spiked into whole blood showing linearity with  $R^2$  value of 0.84. (For interpretation of the references to color in this figure legend, the reader is referred to the web version of this article).

## Acknowledgements

This work was supported by the IDP, TDTD of Department of Science and Technology, India (sanction no. IDP/MED/18/2016). The authors would like to acknowledge the staff at the Centre for NEMS and Nanophotonics (CNNP) at IIT Madras for substrate metallization, the staff at Material Science Research Center (MSRC) at IIT Madras for assistance with acquiring high resolution scanning electron microscopy (HRSEM) images and energy dissipative X-ray (EDAX) data, the Biosensors Laboratory of Dr. Raghavendra Sai at IIT Madras for refractive index measurements, and colleagues in the lab, Sudeepthi Aremanda for fabricating the master mold, Kanchana Pandian for centrifuging blood samples for plasma study, Ravindra Gaikwad for smoothening spectral data using Matlab where required and Butunath Majhy for helpful discussion on capillary flow.

## Conflict of interest

The authors declare no conflict of interest.

## Appendix A. Supporting information

Supplementary data associated with this article can be found in the online version at [doi:10.1016/j.bios.2019.02.036](https://doi.org/10.1016/j.bios.2019.02.036).

## References

- Adegoke, O., Park, E.Y., 2017. Bright luminescent optically engineered core/alloyed shell quantum dots: an ultrasensitive signal transducer for dengue virus RNA via localized surface plasmon resonance-induced hairpin hybridization. *J. Mater. Chem. B* 5, 3047–3058.
- Aeinehvand, M.M., Ibrahim, F., Harun, S.W., Djordjevic, I., Hosseini, S., Rothan, H.A., Yusuf, R., Madou, M.J., 2015. Biosensing enhancement of dengue virus using microballoon mixers on centrifugal microfluidic platforms. *Biosens. Bioelectron.* 67, 424–430.
- Alcon, S., Talarmin, A., Debruyne, M., Falconar, A., Deubel, V., Flamand, M., 2002. Enzyme-linked immunosorbent assay specific to dengue virus type 1 nonstructural protein NS1 reveals circulation of the antigen in the blood during the acute phase of disease in patients experiencing primary or secondary infections. *J. Clin. Microbiol.* 40, 376–381.
- Antunes, P., Watterson, D., Parmvi, M., Burger, R., Boisen, A., Young, P., Cooper, M.A., Hansen, M.F., Ranzoni, A., Donolato, M., 2015. Quantification of NS1 dengue biomarker in serum via optomagnetic nanocluster detection. *Sci. Rep.* 5, 16145.
- Avelino, K.Y.P.S., Andrade, C.A.S., de Melo, C.P., Nogueira, M.L., Correia, M.T.S., Coelho, L.C.B.B., Oliveira, M.D.L., 2014. Biosensor based on hybrid nanocomposite and CramoLL lectin for detection of dengue glycoproteins in real samples. *Synth. Met.* 194, 102–108.
- Bang, J., Park, H., Choi, W., Sung, D., Lee, J.H., Lee, K.Y., Kim, S., 2018. Sensitive detection of dengue virus NS1 by highly stable antibody-functionalized gold nanoparticles. *New J. Chem.* 42, 12607–12614.
- Blacksell, S.D., 2012. Commercial dengue rapid diagnostic tests for point-of-care application: recent evaluations and future needs? *J. Biomed. Biotechnol.* 2012, 1–12.
- Cadamuro, J., Mrazek, C., Leichtle, A.B., Kipman, U., Felder, T.K., Wiedemann, H., Oberkofler, H., Fiedler, G.M., Haschke-Becher, E., 2018. Influence of centrifugation conditions on the results of 77 routine clinical chemistry analytes using standard vacuum blood collection tubes and the new BD-Barricor tubes. *Biochem. Med.* 28, 010704.
- Camara, A.R., Gouvêa, P.M.P., Dias, A.C.M.S., Braga, A.M.B., Dutra, R.F., de Araujo, R.E., Carvalho, I.C.S., 2013. Dengue immunoassay with an LSPR fiber optic sensor. *Opt. Express* 21, 27023–27031.
- Darwish, N.T., Sekaran, S.D., Alias, Y., Khor, S.M., 2018. Immunofluorescence-based biosensor for the determination of dengue virus NS1 in clinical samples. *J. Pharm. Biomed. Anal.* 149, 591–602.
- Dengue: Guidelines for Diagnosis Treatment Prevention and Control (New Edition 2009), 2009. New World Health Organization, France.
- Dias, A.C.M.S., Gomes-Filho, S.L.R., Silva, M.M.S., Dutra, R.F., 2013. A sensor tip based on carbon nanotube-ink printed electrode for the dengue virus NS1 protein. *Biosens. Bioelectron.* 44, 216–221.
- Dutra, R.F., M. Silva, A.C., Saade, J., Guedes, M.I. F., Cordeiro, M.T., 2018. A carbon ink screen-printed immunoelectrode for Dengue virus NS1 protein detection based on photosynthesized amine gold nanoparticles. *J. Electron. Sens.* 1, 1–12.
- Fang, X., Tan, O.K., Tse, M.S., Ooi, E.E., 2010. A label-free immunosensor for diagnosis of dengue infection with simple electrical measurements. *Biosens. Bioelectron.* 25, 1137–1142.
- Faucheux, J.A., Stanton, A.L.D., Jain, P.K., 2014. Plasmon resonances of semiconductor nanocrystals: physical principles and new opportunities. *J. Phys. Chem. Lett.* 5, 976–985.
- Hadis, N.S.M., Manaf, A.A., Ngalm, S.H., Herman, S.H., Sawada, K., Fauzi, N.A., 2017. Fabrication of fluidic-based memristor sensor for dengue virus detection, In: 2017 IEEE Asia Pacific Conference on Postgraduate Research in Microelectronics and Electronics (PrimeAsia). IEEE, pp. 105–108.
- Henglein, A., Meisel, D., 1998. Spectrophotometric observations of the adsorption of organosulfur compounds on colloidal silver nanoparticles. *J. Phys. Chem. B* 102, 8364–8366.
- Hosseini, S., Aeinehvand, M.M., Uddin, S.M., Benzina, A., Rothan, H.A., Yusuf, R., Koole, L.H., Madou, M.J., Djordjevic, I., Ibrahim, F., 2015. Microsphere integrated microfluidic disk: synergy of two techniques for rapid and ultrasensitive dengue detection. *Sci. Rep.* 5, 16485.
- Hu, D., Fry, S., Huang, J., Ding, X., Qiu, L., Pan, Y., Chen, Y., Jin, J., McElnea, C., Buechler, J., Che, X., Cooper, M., Hu, D., Fry, S.R., Huang, J.X., Ding, X., Qiu, L., Pan, Y., Chen, Y., Jin, J., McElnea, C., Buechler, J., Che, X., Cooper, M.A., 2013. Comparison of surface plasmon resonance, resonant waveguide grating biosensing and enzyme linked immunosorbent assay (ELISA) in the evaluation of a dengue virus immunoassay. *Biosensors* 3, 297–311.
- Huang, M.J., Xie, H., Wan, Q., Zhang, L., Ning, Y., Zhang, G.-J., 2013. Serotype-specific identification of dengue virus by silicon nanowire array biosensor. *J. Nanosci. Nanotechnol.* 13, 3810–3817.
- Iswardy, E., Tsai, T.-C., Cheng, I.-F., Ho, T.-C., Perng, G.C., Chang, H.-C., 2017. A bead-based immunofluorescence-assay on a microfluidic dielectrophoresis platform for rapid dengue virus detection. *Biosens. Bioelectron.* 95, 174–180.
- Jahanshahi, P., Zalnezhad, E., Sekaran, S.D., Adikan, F.R.M., 2015. Rapid immunoglobulin m-based dengue diagnostic test using surface plasmon resonance biosensor. *Sci. Rep.* 4, 3851.
- Jenkins, J.A., Zhou, Y., Thota, S., Tian, X., Zhao, X., Zou, S., Zhao, J., 2014. Blue-shifted narrow localized surface plasmon resonance from dipole coupling in gold nanoparticle random arrays. *J. Phys. Chem. C* 118, 26276–26283.
- Kumbhat, S., Sharma, K., Gehlot, R., Solanki, A., Joshi, V., 2010. Surface plasmon resonance based immunosensor for serological diagnosis of dengue virus infection. *J. Pharm. Biomed. Anal.* 52, 255–259.
- Laguna, M., Holgado, M., Sanza, F., Lavín, A., López, A., Casquel, R., Laguna, M.F., Holgado, M., Sanza, F.J., Lavín, A., López, A., Casquel, R., 2014. Optimization of dengue immunoassay by label-free interferometric optical detection method. *Sensors* 14, 6695–6700.
- Lanciotti, R.S., Calisher, C.H., Gubler, D.J., Chang, G.J., Vorndam, A.V., 1992. Rapid detection and typing of dengue viruses from clinical samples by using reverse transcriptase-polymerase chain reaction. *J. Clin. Microbiol.* 30, 545–551.
- Liu, C., Mauk, M., Gross, R., Bushman, F.D., Edelstein, P.H., Collman, R.G., Bau, H.H., 2013. Membrane-based, sedimentation-assisted plasma separator for point-of-care applications. *Anal. Chem.* 85, 10463–10470.
- Mayer, K.M., Hafner, J.H., 2011. Localized surface plasmon resonance sensors. *Chem. Rev.* 111, 3828–3857.
- McDonald, J.C., Whitesides, G.M., 2002. Poly(dimethylsiloxane) as a material for fabricating microfluidic devices. *Acc. Chem. Res.* 35, 491–499.
- Mustapha Kamil, Y., Abu Bakar, M.H., Amir Hamzah, A.S., Yaacob, M.H., Ngee, L.H., Mahdi, M.A., 2018a. Dengue E protein detection using graphene oxide integrated tapered optical fiber sensor. *IEEE J. Sel. Top. Quantum Electron.* 25, 1–8.
- Mustapha Kamil, Y., Abu Bakar, M.H., Mustapa, M.A., Yaacob, M.H., Abidin, N.H.Z., Syahir, A., Lee, H.J., Mahdi, M.A., 2018b. Label-free Dengue E protein detection using a functionalized tapered optical fiber sensor. *Sens. Actuators B Chem.* 257, 820–828.
- Navakul, K., Warakulwit, C., Yenchitsomanus, P., Panya, A., Lieberzeit, P.A., Sangma, C., 2017. A novel method for dengue virus detection and antibody screening using a graphene-polymer based electrochemical biosensor. *Nanomed. Nanotechnol. Biol. Med.* 13, 549–557.
- Nguyen, B.T.T., Peh, A.E.K., Chee, C.Y.L., Fink, K., Chow, V.T.K., Ng, M.M.L., Toh, C.-S., 2012. Electrochemical impedance spectroscopy characterization of nanoporous alumina dengue virus biosensor. *Bioelectrochemistry* 88, 15–21.

- de Oliveira, G.M.F., Farooq, S., Dutra, R.F., de Araujo, R.E., 2017. Engineering of solution-based localized surface plasmon resonance platform for dengue diagnosis. In: 2017 Conference on Lasers and Electro-Optics Europe & European Quantum Electronics Conference (CLEO/Europe-EQEC). IEEE, pp. 1–1.
- Odeh, A.A., Al-Douri, Y., Voon, C.H., Mat Ayub, R., Gopinath, S.C.B., Odeh, R.A., Ameri, M., Bouhemadou, A., 2017. A needle-like Cu<sub>2</sub>CdSnS<sub>4</sub> alloy nanostructure-based integrated electrochemical biosensor for detecting the DNA of Dengue serotype 2. *Microchim. Acta* 184, 2211–2218.
- Oliveira, M.D.L., Nogueira, M.L., Correia, M.T.S., Coelho, L.C.B.B., Andrade, C.A.S., 2011. Detection of dengue virus serotypes on the surface of gold electrode based on Cratylia mollis lectin affinity. *Sens. Actuators B Chem.* 155, 789–795.
- Omar, N.A.S., Fen, Y.W., Abdullah, J., Chik, C.E.N.C.E., Mahdi, M.A., 2018. Development of an optical sensor based on surface plasmon resonance phenomenon for diagnosis of dengue virus E-protein. *Sens. Bio-Sens. Res.* 20, 16–21.
- Ortega, G.A., Pérez-Rodríguez, S., Reguera, E., 2017. Magnetic paper – based ELISA for IgM-dengue detection. *RSC Adv.* 7, 4921–4932.
- Ortega, G.A., Zuaznabar-Gardona, J.C., Reguera, E., 2018. Electrochemical immunoassay for the detection of IgM antibodies using polydopamine particles loaded with PbS quantum dots as labels. *Biosens. Bioelectron.* 116, 30–36.
- Pal, S., Dauner, A.L., Mitra, I., Forshey, B.M., Garcia, P., Morrison, A.C., Halsey, E.S., Kochel, T.J., Wu, S.-J.L., 2014. Evaluation of dengue NS1 antigen rapid tests and ELISA kits using clinical samples. *PLoS One* 9, e113411.
- Parkash, O., Shueb, R.H., 2015. Diagnosis of dengue infection using conventional and biosensor based techniques. *Viruses* 7, 5410–5427.
- Parkash, O., Yean, C., Shueb, R., Parkash, O., Yean, C.Y., Shueb, R.H., 2014. Screen printed carbon electrode based electrochemical immunosensor for the detection of dengue NS1 antigen. *Diagnostics* 4, 165–180.
- Patramool, S., Bernard, E., Hamel, R., Natthanej, L., Chazal, N., Surasombatpattana, P., Ekchariyawat, P., Daoust, S., Thongrungrat, S., Thomas, F., Briant, L., Missé, D., 2013. Isolation of infectious chikungunya virus and dengue virus using anionic polymer-coated magnetic beads. *J. Virol. Methods* 193, 55–61.
- Peeling, R.W., Artsob, H., Pelegrino, J.L., Buchy, P., Cardoso, M.J., Devi, S., Enria, D.A., Farrar, J., Gubler, D.J., Guzman, M.G., Halstead, S.B., Hunsperger, E., Kliks, S., Margolis, H.S., Nathanson, C.M., Nguyen, V.C., Rizzo, N., Vázquez, S., Yoksan, S., 2010. Evaluation of diagnostic tests: dengue. *Nat. Rev. Microbiol.* 8, S30–S37.
- Rajesh, Sharma, V., Mishra, S.K., Biradar, A.M., 2012. Synthesis and electrochemical characterization of myoglobin-antibody protein immobilized self-assembled gold nanoparticles on ITO-glass plate. *Mater. Chem. Phys.* 132, 22–28.
- Sánchez-Purrà, M., Carré-Camps, M., de Puig, H., Bosch, I., Gehrke, L., Hamad-Schifferli, K., 2017. Surface-enhanced Raman spectroscopy-based sandwich immunoassays for multiplexed detection of Zika and Dengue viral biomarkers. *ACS Infect. Dis.* 3, 767–776.
- Silva, M.M.S., Dias, A.C.M.S., Cordeiro, M.T., Marques, E., Goulart, M.O.F., Dutra, R.F., 2014. A thiophene-modified screen printed electrode for detection of dengue virus NS1 protein. *Talanta* 128, 505–510.
- Silva, M.M.S., Dias, A.C.M.S., Silva, B.V.M., Gomes-Filho, S.L.R., Kubota, L.T., Goulart, M.O.F., Dutra, R.F., 2015. Electrochemical detection of dengue virus NS1 protein with a poly(allylamine)/carbon nanotube layered immunoelectrode. *J. Chem. Technol. Biotechnol.* 90, 194–200.
- Souza, E., Nascimento, G., Santana, N., Ferreira, D., Lima, M., Natividade, E., Martins, D., Lima-Filho, J., Souza, E., Nascimento, G., Santana, N., Ferreira, D., Lima, M., Natividade, E., Martins, D., Lima-Filho, J., 2011. Label-free electrochemical detection of the specific oligonucleotide sequence of dengue virus type 1 on pencil graphite electrodes. *Sensors* 11, 5616–5629.
- Sreenivasan, M.G., Malik, S., Thigulla, S., Mehta, B.R., 2013. Dependence of plasmonic properties of silver island films on nanoparticle size and substrate coverage. *J. Nanomater.* 2013, 1–8.
- Tani, T., 2015. Light absorption and scattering of Ag and metal nanoparticles. In: *Silver Nanoparticles*. Oxford University Press, pp. 109–140.
- Velez, M., Kuno, G., Gubler, D.J., Oliver, A., Sather, G.E., 1984. Mosquito cell cultures and specific monoclonal antibodies in surveillance for dengue viruses. *Am. J. Trop. Med. Hyg.* 33, 158–165.
- Wang, M., Pan, N., 2008. Predictions of effective physical properties of complex multi-phase materials. *Mater. Sci. Eng. R. Rep.* 63, 1–30.
- Wasik, D., Mulchandani, A., Yates, M.V., 2018. Point-of-use nanobiosensor for detection of dengue virus NS1 antigen in Adult *Aedes aegypti*: a potential tool for improved dengue surveillance. *Anal. Chem.* 90, 679–684.
- Weng, C.-H., Huang, T.-B., Huang, C.-C., Yeh, C.-S., Lei, H.-Y., Lee, G.-B., 2011. A suction-type microfluidic immunosensing chip for rapid detection of the dengue virus. *Biomed. Microdevices* 13, 585–595.
- Wong, W.R., Krupin, O., Sekaran, S.D., Mahamd Adikan, F.R., Berini, P., 2014. Serological diagnosis of dengue infection in blood plasma using long-range surface plasmon waveguides. *Anal. Chem.* 86, 1735–1743.
- Wong, W.R., Sekaran, S.D., Mahamd Adikan, F.R., Berini, P., 2016. Detection of dengue NS1 antigen using long-range surface plasmon waveguides. *Biosens. Bioelectron.* 78, 132–139.
- Zaytseva, N.V., Goral, V.N., Montagna, R.A., Baumner, A.J., 2005. Development of a microfluidic biosensor module for pathogen detection. *Lab Chip* 5, 805–811.